IOPscience iopscience.iop.org

Home Search Collections Journals About Contact us My IOPscience

Light impurity effects on the electronic structure in TiAl

This article has been downloaded from IOPscience. Please scroll down to see the full text article.

2006 J. Phys.: Condens. Matter 18 8803

(http://iopscience.iop.org/0953-8984/18/39/011)

View the table of contents for this issue, or go to the journal homepage for more

Download details:
IP Address: 129.252.86.83
The article was downloaded on 28/05/2010 at 14:07

Please note that terms and conditions apply.

INSTITUTE OF PHYSICS PUBLISHING JOURNAL OF PHYSICS: CONDENSED MATTER

J. Phys.: Condens. Matter **18** (2006) 8803–8815 doi:10.1088/0953-8984/18/39/011

Light impurity effects on the electronic structure in TiAl

H L Dang[1], C Y Wang[1,2,3] and T Yu[1]

[1] Central Iron and Steel Research Institute, Beijing 100081, People's Republic of China
[2] Department of Physics, Tsinghua University, Beijing 100084, People's Republic of China
[3] International Center for Materials Physics, Academica, Shenyang 110016, People's Republic of China

E-mail: hongli_dang@163.com

Received 24 April 2006, in final form 5 July 2006
Published 11 September 2006
Online at stacks.iop.org/JPhysCM/18/8803

Abstract

By using first-principles DMol and the discrete-variational method (DVM) based on density functional theory, we investigated the effect of some light impurities, H, B, C, N and O, on the electronic structure of their corresponding different impurity-doped systems in γ-TiAl. The impurity formation energy, Mulliken occupation, bond order and charge density difference have been calculated to study the impurity-induced changes in the energetics and electronic structure. According to the impurity formation energy, it is found that the impurities energetically prefer to occupy the Ti-rich octahedron interstitial sites in the order H < B < O < N < C. Charge transfer suggests that the effect of the impurities is localized and the bond order as well as charge density difference results show that B, C and N are beneficial for the ductility of TiAl, while H and O are not.

(Some figures in this article are in colour only in the electronic version)

1. Introduction

Having a simple crystal structure, low density and high melting temperature, intermetallic $L1_0$-ordered TiAl is of interest as one of the candidate high-temperature materials for the next generation. However, it still suffers from a lack of low-temperature ductility and a lack of high-temperature strength [1–4]. Alloying with a third element and microstructural modifications through thermomechanical treatments are essential for the further improvement of room-temperature ductility as well as the high-temperature strength of TiAl. In addition to a third element, many trace elements and minor alloying additions may be present (by accident or design) in γ-TiAl. These impurities and trace elements, including H, B, C, N and O, etc, can dramatically affect the strength and the ductility of high-temperature materials [5–7]. A

well-known example is that microalloying with boron can sharply increase the ductility and meanwhile effectively suppress the intergranular fracture in polycrystalline Ni_3Al [8].

Kawabata *et al* [9] has revealed that the mechanical properties of TiAl are improved by optimum additions of interstitial elements such as carbon, boron and nitrogen. Preliminary experimental and theoretical studies were carried out within TiAl structure either by inserting or by substituting carbon [10–13]. Theoretically, physical properties such as the change of brittleness can be addressed starting from the results of *ab initio* self-consistent calculations. Boron addition in lamellar TiAl alloys has a significant effect on room-temperature tensile ductility, for example ∼0.8 at.% boron additions have been shown to be very beneficial for refining the lamellar colony in cast material [14–16]. The remarkable reduction in lamellar size has significant effects on thermomechanical processing properties, such as forging and extrusion, improving deformation homogeneity, and the surface quality of parts. In addition, minor additions of boron have been shown to stabilize lamellar structure and change the brittle-to-ductility transition temperature of a given alloy [17]. As the effects of boron on refining and stabilizing lamellar structure improve ductility, strength and creep resistance, it is important to understand the effects of boron on α to $\alpha_2 + \gamma$ transformation during continuous cooling and mechanical properties.

Among alloying elements, nitrogen is known to be important, because it can be absorbed easily from the atmosphere during melting or heat-treatments and is expected to affect the ductility and strength of TiAl. Yuki *et al* [18] have investigated the effect of nitrogen addition on the mechanical properties of case γ-TiAl alloys and revealed that both the room-temperature ductility and the strength increase with increasing nitrogen content up to 0.3 mass%. They concluded that the improvement in room-temperature mechanical properties is mainly caused by grain refinement and precipitation hardening.

It has been speculated that oxygen depletion changes the deformation mechanism and increases the ductility [19, 20]. In single-phase γ, interstitial oxygen can be lowered by the addition of Er to form oxide [21]. More recent experiments indicated directly that the yield stress increases but room-temperature ductility decreases with oxygen content in alloys [22, 23]. The above facts suggest that the investigation of the embrittlement mechanism induced by oxygen is significant both scientifically and technically. The determination of the oxygen embrittlement of TiAl at the electronic level through many theoretical efforts has been devoted to bulk TiAl or the defect systems in TiAl [24, 25]. The competition in occupation between oxygen and hydrogen, which has crucial effects on environmental embrittlement, was also discussed in Liu's study [26].

From the above, it is found that, although considerable theoretical efforts have been devoted to the investigation of the fundamental mechanisms underlying these impurity effects on the TiAl system, not many systematic theoretical calculations have been carried out up to now, which is significant in understanding the strengthening mechanism in TiAl-based superalloys. To this end, we have carried out systematic first-principles energy and electronic structure calculations on TiAl using DMol [27, 28] and the discrete variational method (DVM) [29–31] based on density functional theory. This will contribute towards understanding the electronic mechanism underlying the contrasting effects of the beneficial and detrimental elements on these high-temperature structural materials. In section 2, we briefly describe the cluster model and methods used in this paper. To identify the interstitial site occupation preferentially for the light elements (such as H, B, C, N and O), we calculated the impurity formation energy of impurity-doped TiAl in section 3.1. The pure (clean) and impurity-doped TiAl systems are investigated in detail using the Mulliken population, bond order, and charge density difference in sections 3.2–3.4, respectively. Finally, a brief summary is given in section 4.

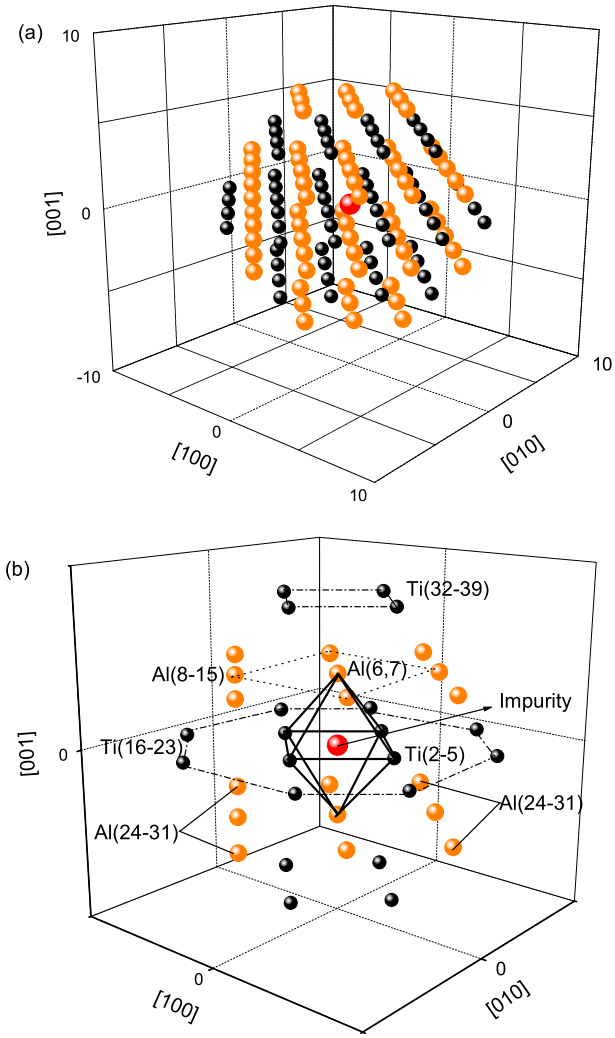

Figure 1. (a) The cluster model used in the calculation; (b) the tab of some particular atoms. The smaller spheres, larger spheres and the largest sphere present the Ti atoms, Al atoms and impurity atom in the Ti-rich octahedral interstitial site (A) as well as the Al atoms, Ti atoms and impurity atom in the Al-rich case (B), respectively.

2. The computation method and cluster model

The discrete variational method (DVM), which is a first-principles numerical method for solving the Kohn–Sham equations, has been used successfully to study the electronic structure of metals, alloys and intermetallic compound etc [32–34]. In this paper, the electronic structure and doping effect of γ-TiAl are calculated.

It is well known that γ-TiAl has a face-centred tetragonal (fct) $L1_0$ crystal structure with alternate (001) planes of Ti and Al atoms. We first perform a series of total energy calculations using different lattice constants to determine the lattice constant for the TiAl system. The calculated a, c and tetragonality of the γ-TiAl corresponding to the lowest binding energy are 3.992 Å, 4.072 Å and 1.020, respectively, which are very close to the experimental values of

3.99 Å, 4.07 Å and 1.02 [35]. Thus we construct the initial atomic configuration of γ-TiAl with a and c being 3.99 and 4.07 Å, from which we extract a cluster model with 132 atoms for the first-principles calculation, which is illustrated in figure 1(a). For convenient analysis, in figure 1(b) we have labelled some particular atoms with the Arabic numerals. Because the atomic radii of the light elements (X) are smaller than that of the Ti or Al atom, these X atoms in γ-TiAl should be introduced into the interstitial sites rather than substituted for Ti or Al atoms for the purpose of studying the electronic effect of TiAl with the impurity. Based on previous studies, we have placed the light impurities in the octahedral interstitial site in impurity-doped systems [26]. The pure TiAl and TiAl–X (X = H, B, C, N, and O) clusters are used to simulate the dopant-free (clean) and X-doped TiAl systems, respectively.

The size and the electronic configuration of the impurity and the host atoms are different, therefore the local distortion will be induced when an impurity is doped into γ-TiAl system. In order to obtain an equilibrium atomic configuration, the DMol method that can provide the energy gradient for each atom is used to optimize the local structure. Considering the short-range effect for the impurity, only the impurity and its first-nearest-neighbouring (FNN) as well as the second-nearest-neighbouring (SNN) atoms are allowed to relax and all other atoms are fixed at their ideal host positions to keep the preservation of the D_{4h} symmetry. In the DMol calculations, the convergence criteria for the energy gradient and the atomic displacement are, respectively, 5×10^{-4} Ryd Å^{-1} and 5×10^{-4} Å. Non-spin-polarized wavefunctions are used, as the authors are mainly concerned with the structure and related mechanical properties. The double numerical polarized (DNP) basis, including the inner orbitals and the exchange–correlation functional, is chosen with the Perdew–Burke–Ernzerhof general gradient approximation (GGA) correction [36] in order to obtain more precise results.

To use the real-space cluster method, one must guarantee that the cluster size is large enough to eliminate the surface effect for inner atoms. Hence, we have carefully tested the effect of the cluster size on the impurity formation energies and found that the impurity formation energy calculated will be insensitive to the cluster size if the number of atoms reaches and exceeds some amount. Considering the reliable impurity formation energy and the calculation time spent, we have chosen the 132-atom cluster model in the present paper. The model size has been proved to be reasonable through the work of Song *et al* [37], where it shows that only the SNN atoms included in the clusters will ensure the accuracy of the calculated binding energy.

3. Results and discussion

3.1. Impurity formation energy

In order to study the effect of the local environment of the impurity on the electronic structure, it is necessary to identify the interstitial site that the impurity atom prefers to occupy. We have considered two different types of octahedral sites shown in figure 1 and calculated the impurity formation energy (IFE) as follows [26]:

$$\begin{aligned}\Delta E_{\mathrm{imp}} &= E_{\mathrm{tot}}(\mathrm{TiAl–X}) - E_{\mathrm{tot}}(\mathrm{TiAl}) - E_{\mathrm{tot}}(\mathrm{X}) \\ &= \{E_{\mathrm{tot}}(\mathrm{TiAl–X}) - [E_{\mathrm{tot}}(\mathrm{Ti}) + E_{\mathrm{tot}}(\mathrm{Al}) + E_{\mathrm{tot}}(\mathrm{X})]\} \\ &\quad - \{E_{\mathrm{tot}}(\mathrm{TiAl}) - [E_{\mathrm{tot}}(\mathrm{Ti}) + E_{\mathrm{tot}}(\mathrm{Al})]\} \\ &= E_{\mathrm{b}}(\mathrm{TiAl–X}) - E_{\mathrm{b}}(\mathrm{TiAl}) \qquad (1)\end{aligned}$$

where E_{tot}(TiAl–X) is the total energy of the cluster with the impurity X lying at a certain octahedral site, E_{tot}(TiAl) is the total energy of the cluster without the impurity. E_{tot}(Ti), E_{tot}(Al) and E_{tot}(X) are the total energies of an isolated Ti, Al and X atom, respectively, and E_{b}(TiAl–X) and E_{b}(TiAl) are the binding energies of the corresponding clusters, respectively.

Table 1. Impurity formation energies (in eV) of the light impurity atoms at two different types of octahedral interstitial sites.

Octahedral interstitial sites	H	B	C	N	O
A	−2.34	−5.90	−8.09	−6.97	−6.69
B	−1.73	−4.85	−6.44	−5.17	−5.14

The IFEs of X atoms in different impurity cases at two different types of octahedral sites are listed in table 1, showing that the IFE varies with the impurity atom type and the environment. It can also be found from table 1 that all the IFEs at the Ti-rich octahedral interstitial site A are much more negative than those at the Al-rich octahedral interstitial site B. Thus we consider that all the impurities are energetically favourable to occupy the Ti-rich octahedral site rather than the Al-rich site. This may be reasonable, regarding that there will be a larger charge carried by the impurity when it is placed near Ti than in the neighbourhood of Al, which points to a relatively larger stabilization of the lattice in such a configuration. Therefore, the following electronic structure studies are carried out only when an X atom is placed into the Ti-rich octahedral interstitial site.

From table 1 we can also find that the IFE in the Ti-rich case decreases (less negative) in the order of H < B < O < N < C, which suggests that the trend for the impurity occupies the Ti-rich octahedron interstitial sites in the same order. This trend can provide us with a criterion for impurity occupation competition. For example, the IFE results show that oxygen has a stronger occupation tendency compared with hydrogen, i.e. oxygen proceeds to occupy the Ti-rich octahedron interstitial sites when oxygen and hydrogen both exist. This indicates that oxygen in TiAl can effectively suppress the hydrogen permeation. Hydrogen is known to induce environment embrittlement [38] and then we can conclude that the higher the oxygen content in TiAl, the less sensitive it is to the environmental loss in ductility caused by hydrogen. This conclusion is consistent with the experimental and theoretical results [26, 39].

3.2. Mulliken population

Mulliken populations [40] can reflect the electron transfer among the different atoms and orbitals, and help us to analyse the interatomic interactions. Table 2 lists the Mulliken population of every valence orbital of the impurity atoms and the host Ti2–5, Al6–7, Al8–15, Ti16–23, Al24–31, and Ti32–39 atoms etc.

It can be found that H, B, C, N and O all gain electrons from the adjacent host atoms, and most of these electrons are concentrated in the 2p orbitals (except for the H atom and the 2s orbitals also devote some electrons to the 2p orbitals), which reflects the quantum effect on trapping a light impurity for the Ti-rich octahedral interstitial site in TiAl. Moreover, the s orbital of an impurity loses some electrons. From table 2 we can also find that, for the B, C, N and O doped systems, although the total valence electrons of these impurity atoms increase with increasing atomic number, the electrons that they gain are decreased, which is contradictory to Pauling's electronegativity trend. On the other hand, the adjacent host atoms of the FNN atoms such as Ti2–5, Al6–7 atoms etc generally lose electrons, while the SNN and the third-nearest-neighbouring (TNN) atoms such as Al8–15, Ti16–23 atoms etc gain a small number of electrons. It should be noted that there is very little change in the charge of these TNN host atoms. The charge transfer listed in table 2 indicates that the effect of impurities is localized. It can also be found that the 2p and 3s orbitals of the impurities (except H) gain some electrons from the 3d, 4s orbitals of the FNN Ti atoms and 3s, 3p orbitals of the FNN Al atoms, which indicates that there is a strong hybridization between the impurity-s, p orbitals and the adjacent Ti-3d, 4s and Al-3s, 3p orbitals.

Table 2. Mulliken populations of valence orbitals of the light impurity atoms and their first-nearest-neighbouring as well as the second-nearest-neighbouring and third-nearest-neighbouring atoms in the pure TiAl system and the impurity-doped TiAl systems, where Q is the summation of the populations in all orbitals of the atom, and n and n_0 are the populations of the atoms in the doped and clean cluster, respectively. $\Delta n = n - n_0$.

		Clean	TiAl–H		TiAl–B		TiAl–C		TiAl–N		TiAl–O	
		n_0	n	Δn	n	Δn	n	Δn	n	Δn	n	Δn
Impurity	2s(1s)		1.351	0.351	1.173	−0.827	1.402	−0.598	1.603	−0.397	1.764	−0.236
	2p(2s)		0.053	0.053	2.822	1.822	3.451	1.451	4.074	1.074	4.741	0.741
	3s				0.036	0.036	0.056	0.056	0.083	0.083	0.094	0.094
	Q			0.404		1.031		0.909		0.760		0.599
Ti(2-5)	3d	2.448	2.453	0.005	2.398	−0.050	2.399	−0.049	2.407	−0.041	2.418	−0.030
	4s	0.585	0.525	−0.060	0.433	−0.152	0.449	−0.136	0.456	−0.129	0.470	−0.115
	4p	0.372	0.317	−0.055	0.348	−0.024	0.364	−0.008	0.374	0.002	0.375	0.003
	Q	3.405	3.295	−0.110	3.179	−0.226	3.212	−0.193	3.237	−0.168	3.263	−0.142
Al(6-7)	3s	1.378	1.331	−0.047	1.232	−0.146	1.247	−0.131	1.271	−0.107	1.309	−0.069
	3p	2.203	2.126	−0.077	2.029	−0.174	2.022	−0.181	2.013	−0.190	1.993	−0.210
	Q	3.581	3.457	−0.124	3.261	−0.320	3.269	−0.312	3.284	−0.297	3.302	−0.279
Al(8-15)	3s	1.404	1.405	0.001	1.406	0.002	1.407	0.003	1.407	0.003	1.407	0.003
	3p	2.154	2.178	0.024	2.167	0.013	2.177	0.023	2.183	0.029	2.186	0.032
	Q	3.558	3.583	0.025	3.573	0.015	3.584	0.026	3.590	0.032	3.593	0.035
Ti1(16-23)	3d	2.443	2.451	0.008	2.459	0.016	2.459	0.016	2.460	0.017	2.462	0.019
	4s	0.617	0.618	0.001	0.634	0.017	0.632	0.015	0.629	0.012	0.627	0.010
	4p	0.359	0.351	−0.008	0.340	−0.019	0.339	−0.020	0.339	−0.020	0.340	−0.019
	Q	3.419	3.420	0.001	3.433	0.014	3.430	0.011	3.428	0.009	3.429	0.010

Table 2. (Continued.)

		Clean	TiAl–H		TiAl–B		TiAl–C		TiAl–N		TiAl–O	
		n_0	n	Δn	n	Δn	n	Δn	n	Δn	n	Δn
Al(24-31)	3s	1.419	1.421	0.002	1.420	0.001	1.420	0.001	1.420	0.001	1.421	0.002
	3p	2.158	2.165	0.007	2.179	0.021	2.174	0.016	2.170	0.012	2.169	0.011
	Q	3.577	3.586	0.009	3.599	0.022	3.594	0.017	3.590	0.013	3.590	0.013
Ti(32-39)	3d	2.471	2.472	0.001	2.481	0.010	2.481	0.010	2.481	0.010	2.482	0.011
	4s	0.645	0.647	0.002	0.649	0.004	0.651	0.006	0.652	0.007	0.651	0.006
	4p	0.421	0.427	0.006	0.432	0.011	0.432	0.011	0.431	0.010	0.429	0.008
	Q	3.537	3.546	0.009	3.562	0.025	3.564	0.027	3.564	0.027	3.562	0.025

3.3. Bond order

The bond order (BO) of the overlap population of the electrons between atoms is a measure of the strength of the covalent bonding. Generally, when impurity atoms reside in the interstitial sites in bulk or defect systems, the impurity–metal bond forms and the surrounding metal–metal bond is changed. To describe this impurity-induced cohesion change quantitatively, Liu *et al* [26, 41] developed a new concept, local environmental total bond order (LTBO), which is defined as the sum of all metal–metal and impurity–metal bond orders involved in a local impurity environment. LTBO is reasonable in estimating the cohesive properties of the local impurity environment. A larger LTBO indicates stronger cohesion and better ductility of the system. In the present paper, the impurity FNN octahedron is chosen as the local impurity environment. The calculated LTBOs for pure and impurity-doped systems are presented in figure 2(a); in addition, the BO between the FNN Ti, Al and impurities with variation in the atom order of the impurity elements in impurity-doped systems are presented in figure 2(b).

From figure 2(a) it is found that the LTBO of a clean octahedron decreases due to H and O addition, while it increases due to B, C and N addition. This shows the decohesion effect of H and O and the incohesion effect of B, C, and N on the local environment. This again supports the conclusion that H and O are embrittling elements when placed at the interstitial site of TiAl. From figure 2(b) we find that the BOs of the impurity–FNN host atoms (such as Ti(2) and Al(6)) vary similarly to LTBO. In particular, B, C, N, and O have fairly high impurity–FNN BOs and not very low FNN Ti–Ti and Ti–Al BOs, which finally results in the high LTBO, as shown in figure 2(a). It should be noted that, although the FNN Ti–Ti and Ti–Al BOs in the H case are the highest, the impurity–FNN BOs is lowest, which also leads to the lowest LTBO. This means that, although H can slightly increase the FNN Ti–Ti and Ti–Al bonding, the H–FNN bonding is the weakest.

3.4. Charge density difference

As an important quantity for analysing the bonding character, the charge density difference is obtained by subtracting the electron density of free atoms at the superposition from that of the cluster system. The charge density difference contour maps on the (001) Ti layer of pure and impurity-doped TiAl are plotted in figures 3 and 4(a)–(e). Here, solid and dotted curves represent contours of increased (accumulation) and decreased (depletion) electronic charge density.

In order to further investigate the spatial redistribution of electrons induced by impurity, we have also drawn the second charge density difference [42] in figures 5(a)–(e), which is obtained by subtracting the superimposed electron density of pure TiAl from the corresponding doped system. For comparison, we called the charge density difference of the doped system with the electron density of pure TiAl as the first charge density difference. From the second charge density difference we can clearly see the impurity-induced charge redistribution. For convenience, the same contour levels are used in all different cases. Figure 3 is the charge density difference of the (001) Ti layer in pure TiAl for the comparison with the impurity-doped systems. It shows obvious anisotropic electron density, which arises from the strong directional d–d bonding between the Ti atoms. It had been demonstrated that this anisotropy of charge density distribution induced by d–d Ti directional bonding is among the factors responsible for the poor ductility of γ-TiAl [12, 25, 43].

In figures 4 and 5, one can see the build-up of interstitial charge accumulation between the impurity X atoms and their FNN host Ti atoms, indicating the enhancement in the bonding

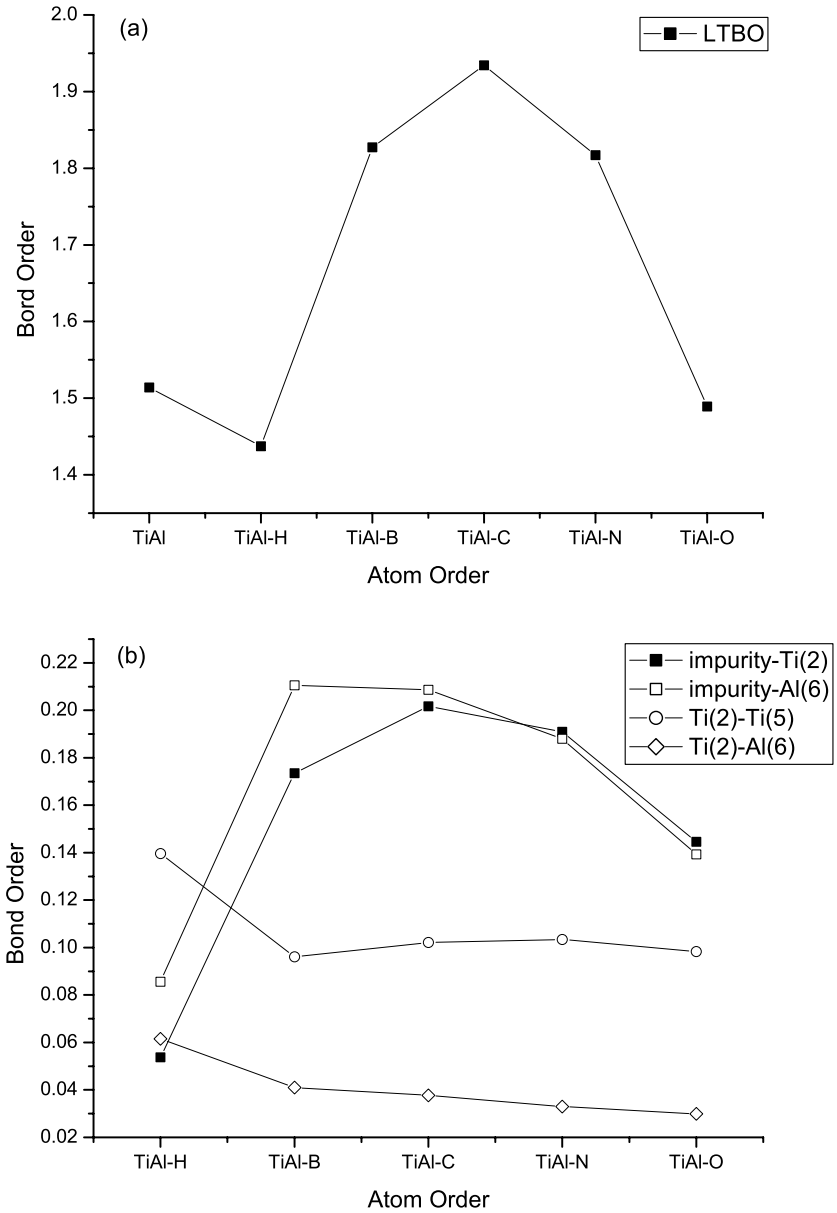

Figure 2. (a) Local environmental total bond order with variation in pure TiAl and impurity atom order; (b) bond order between the first-nearest-neighbouring Ti, Al and impurities with variation in impurity atom order.

between them. Strong electron accumulation is found in the region between B, C, N and O and their FNN Ti atoms, indicating the strong Ti–B, C, N, and O bond. Mulliken population analysis shows that Ti–d/B, C, N, and O-p hybridization contributes dominantly to the strong Ti–B, C, N, and O bonding. It should be noted that the situation is very different in the case of H-doped TiAl, where there is less interstitial charge (almost no bond exists) between H and

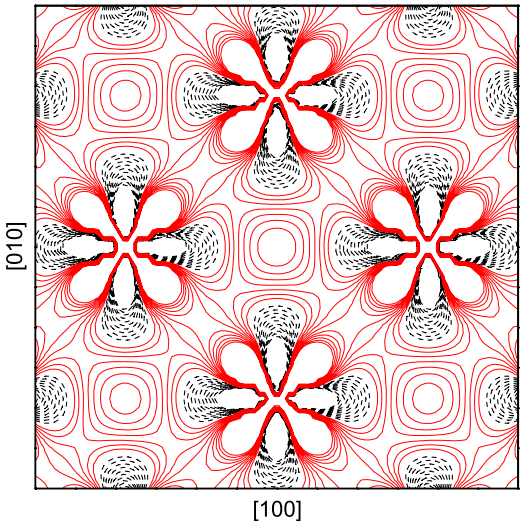

Figure 3. The charge density difference of the (001) Ti layer of the pure TiAl system. The contour spacing is $0.001e$ au^{-3}. Solid and dashed lines correspond to the gain and the loss of electrons, respectively.

its FNN Ti atoms, which also confirms that the Ti–H bonding is the weakest, as in the previous bond order analysis.

As can be seen from the figures for the impurity-doped systems, there is an obvious common feature of significant charge redistribution around the Ti sites. For the B-, C-and N-doped systems, there is an obvious Ti–Ti directional bonding between the nearest Ti atoms, which shows that adding these impurities increases the directionality of the Ti–Ti bonding. But for the H- and O-doped systems, the in-plane d–d bonding was weakened. Based on Morinaga's investigation [12], we can regard that B, C and N are beneficial for the ductility of TiAl, while H and O are not. These results are consistent with other experimental and theoretical results mentioned in the introduction.

4. Summary

Based on the DMol and discrete variational method (DVM) within the framework of density functional theory, we have investigated the electronic structure of several different impurity-doped systems such as H, B, C, N and O in γ-TiAl. Our results show that the impurity formation energy in the Ti-rich case decreases (less negative) in the order of H $<$ B $<$ O $<$ N $<$ C, which suggests the trend for the impurity to occupy the Ti-rich octahedron interstitial sites in the same order. This trend provides us with a criterion for the competition in impurity occupation. The calculated charge transfer suggests that the effect of the impurities is localized. For the B-, C-, N- and O-doped systems, it is interesting that, although the total number of valence electrons of these impurity atoms increases with increasing atomic number, the number of electrons they receive relative to the free states is decreased, which is contradictory to Pauling's electronegativity scale. The bond order and the charge density difference results are also present in this paper. It is found that B, C and N increase the directionality of the in-plane Ti/d–Ti/d bonding while H and O decrease the d–d bonding, which means that B, C and N are beneficial for the ductility of TiAl while H and O are not.

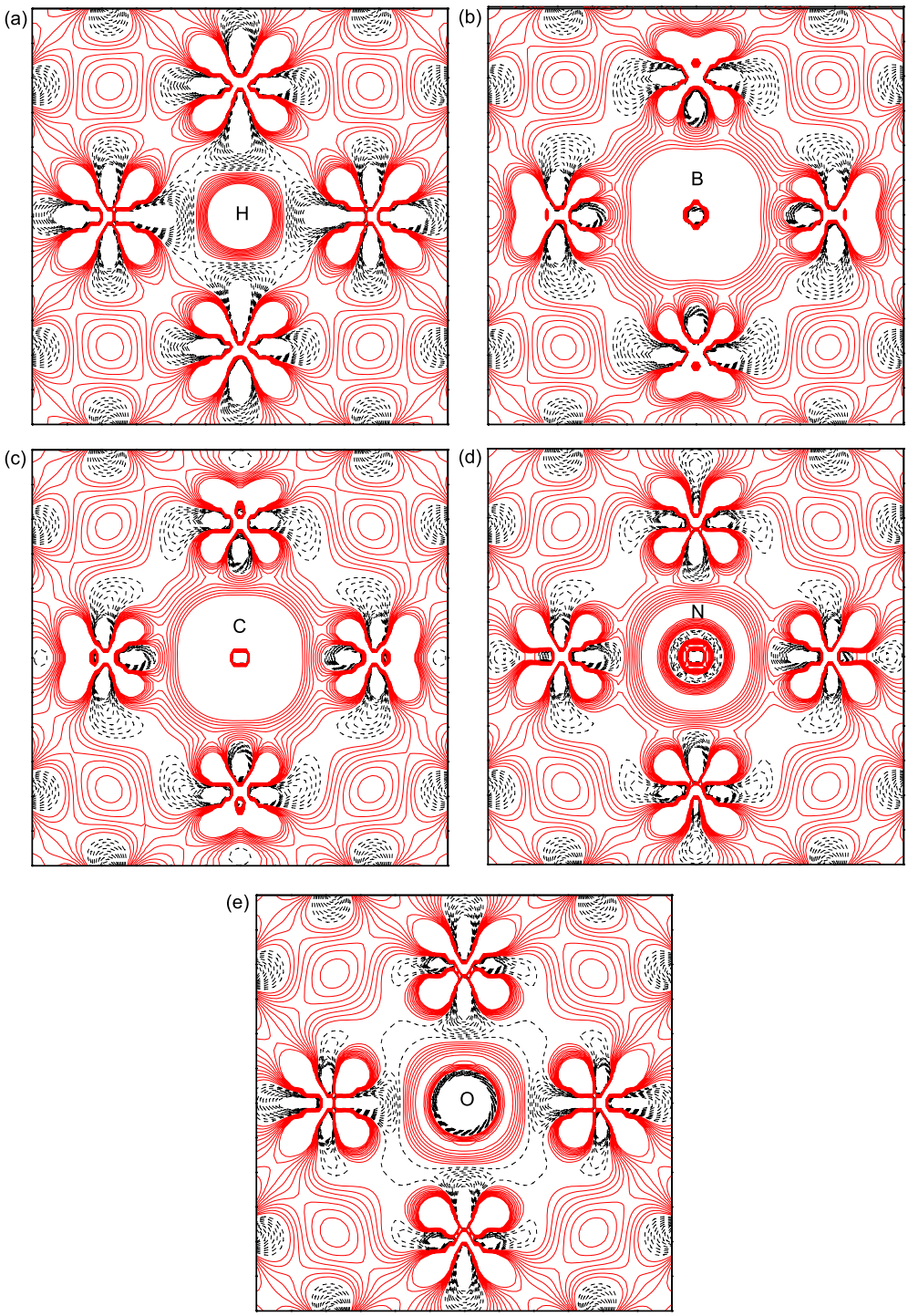

Figure 4. The first charge density difference of the (001) Ti layer of the impurity-doped TiAl system; figures (a)–(e) are for H-, B-, C-, N-, and O-doped TiAl systems, respectively. The contour spacing is $0.001e$ au^{-3}. Solid and dashed lines correspond to the gain and the loss of electrons.

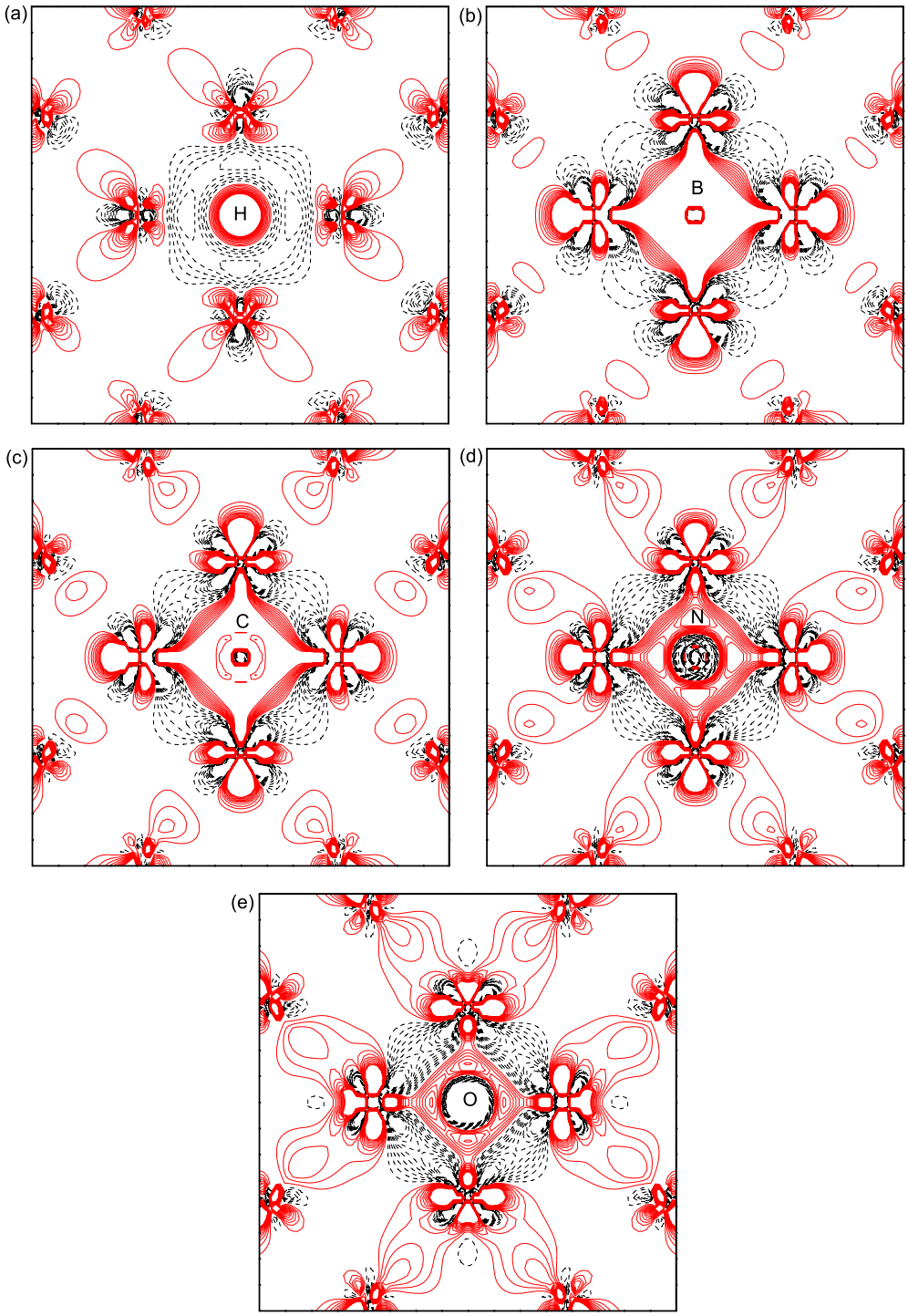

Figure 5. The second charge density difference of the (001) Ti layer of the impurity-doped TiAl system; figures (a)–(e) are for H-, B-, C-, N-, and O-doped TiAl systems, respectively. The contour spacing is $0.001e$ au^{-3}. Solid and dashed lines correspond to the gain and the loss of electrons.

Acknowledgments

One of the authors (Dr H L Dang) is grateful to Dr T Zhu, P F Guan and Z Z Chen for their kind help and beneficial discussion. This research was supported by the '973' Project of the Ministry of Science and Technology of China (Grant No 2006CB605102) and the National Natural Science Foundation of China (Grant No 90306016).

References

[1] Huang S C and Hall E L 1991 *Metall. Trans.* A **22** 427
[2] Kim Y W 1994 *J. Met.* **46** 30
[3] Loria E A 2001 *Intermetallics* **9** 997
[4] Tian W H and Nemoto M 2005 *Intermetallics* **13** 1030
[5] Liu Y, Chen K Y, Lu G, Zhang J H and Hu Z Q 1997 *Acta Mater.* **45** 1837
[6] Holt R T and Wallace W 1976 *Int. Met. Rev.* **1** 203
[7] Bieber C G and Decker R F 1961 *Trans. AIME* **221** 629
[8] Aoki K and Izumi O 1979 *Nippon Kinzoku Gakkaish* **43** 1190
[9] Kawabata T, Tadana M and Izumi O 1991 *ISIJ Int.* **31** 1161
[10] Matar S F, Petitcorps Y L and Etourneau J 1998 *Comput. Mater. Sci.* **10** 314
[11] Vujic D, Li Z and Wang S H 1988 *Metall. Trans.* **19** 2445
[12] Morinaga M, Saito J, Yukawa N and Adach H 1990 *Acta Metall. Mater.* **38** 25
[13] Chubb S R, Papaconstantopoulos D A and Klein B M 1988 *Phys. Rev.* B **38** 120
[14] Graef M D, Hardwick D A and Martin P L 1997 *Structural Intermetallics* ed M V Nathal, R Darolia, C T Liu, P L Martin, D B Miracle, R Wagner and M Yamaguchi (Warrendale, PA: TMS) p 185
[15] Krishnan M, Nalarajan B, Vasudevan V K and Dimiduk M 1997 *Structural Intermetallics* ed M V Nathal, R Darolia, C T Liu, P L Martin, D B Miracle, R Wagner and M Yamaguchi (Warrendale, PA: TMS) p 235
[16] Cheng T T 2000 *Intermetallics* **8** 29
[17] Liu T L, Wang Y, Liu J L and Law C C 1999 *High-Temperature Ordered-Intermetallics Alloys V* ed E P George, M J Mills and M Yamaguchi (Pittsburgh, PA: MRS) p KK2.7.1
[18] Yuki I, Amino N, Uzumi M, Inui H and Yamaguchi M 1994 *J. Japan Inst. Met.* **58** 564
[19] Huang S C and Hall E L 1991 *Metall. Trans.* **5** 1373
[20] Kawabata T, Tadano M and Izumi O 1988 *Scr. Metall.* **22** 1725
[21] Vasudevan V K, Court S A, Kurath P and Fraser H L 1989 *Scr. Metall.* **23** 467
[22] Murata Y, Morinaga M and Takeda Y 1992 *Mater. Trans.* **33** 419
[23] Yamauchi S and Shiraish H 1992 *Mater. Sci. Eng.* A **152** 283
[24] Woodward C, MacLaren J M and Rao S 1992 *J. Mater. Res.* **7** 1735
[25] Song Y, Tang S P, Xu J H, Mryasov O N, Freeman A J, Woodward C and Dimiduk D M 1994 *Phil. Mag.* B **70** 987
[26] Liu Y, Chen K Y, Zhang J H, Hu Z Q, Lu G and Kioussis N 1997 *J. Phys.: Condens. Matter* **9** 9829
[27] Delley B 1990 *J. Chem. Phys.* **92** 508
[28] Delley B 1991 *J. Chem. Phys.* **94** 7245
[29] Painter G S and Ellis D E 1970 *Phys. Rev.* B **1** 4747
[30] Delley B and Ellis D E 1982 *J. Chem. Phys.* **76** 1949
[31] Guenzburger D and Ellis D E 1992 *Phys. Rev.* B **45** 285
[32] Wang C Y 1995 *Defect Diffus. Forum* **79** 125
[33] Wang F H, Wang C Y and Yang J L 1996 *J. Phys.: Condens. Matter* **8** 5527
[34] Wang F H and Wang C Y 1998 *Phys. Rev.* B **57** 289
[35] Brandes E A 1983 *Smithells' Metals Reference Book* 6th edn (London: Butterworth)
[36] Perdew J P, Burke K and Ernzerhof M 1996 *Phys. Rev. Lett.* **77** 3865
[37] Song Y, Yang R, Li D, Hu Z Q and Guo Z X 2000 *Intermetallics* **8** 563
[38] Nakamura M, Hashimoto K and Tsujimoto T 1993 *J. Mater. Res.* **8** 68
[39] Wang D 1995 *PhD Thesis* Shanghai Jiaotong University
[40] Mulliken R S 1955 *J. Chem. Phys.* **23** 1833
[41] Liu Y, Chen K Y, Lu G, Zhang J H and Hu Z Q 1997 *Acta Mater.* **45** 1837
[42] Dang H L, Wang C Y and Shu X L 2004 *Prog. Nat. Sci.* **14** 477
[43] Greenberg B F, Anisimov V I, Gornostirev Y N and Taluts G G 1988 *Scr. Metall.* **22** 859